Disruption of ferroportin 1 regulation causes dynamic alterations in iron homeostasis and erythropoiesis in polycythaemia mice

Henry Mok[1], Jaroslav Jelinek[2,*], Sonia Pai[1], Bruce M. Cattanach[3], Josef T. Prchal[2], Hagop Youssoufian[1,†] and Armin Schumacher[1,‡]

[1]Department of Molecular and Human Genetics, Baylor College of Medicine, Houston, TX 77030, USA
[2]Department of Medicine, Baylor College of Medicine, Houston, TX 77030, USA
[3]MRC Mammalian Genetics Unit, Medical Research Council, Harwell, Oxfordshire OX11 0RD, UK
*Present address: Department of Leukemia, University of Texas M.D. Anderson Cancer Center, Houston, TX 77030, USA
†Present address: Aventis Pharmaceuticals, Bridgewater, NJ 08807, USA
‡Author for correspondence (e-mail: armins@bcm.tmc.edu)

Development 131, 1859-1868
Published by The Company of Biologists 2004
doi:10.1242/dev.01081

Accepted 13 January 2004

Summary

Coding region mutations in the principal basolateral iron transporter of the duodenal enterocyte, ferroportin 1 (FPN1), lead to autosomal dominant reticuloendothelial iron overload in humans. We report the positional cloning of a hypermorphic, regulatory mutation in *Fpn1* from radiation-induced polycythaemia (*Pcm*) mice. A 58 bp microdeletion in the *Fpn1* promoter region alters transcription start sites and eliminates the iron responsive element (IRE) in the 5′ untranslated region, resulting in increased duodenal and hepatic Fpn1 protein levels during early postnatal development. *Pcm* mutants, which are iron deficient at birth, exhibited increased Fpn1-mediated iron uptake and reticuloendothelial iron overload as young adult mice. Additionally, *Pcm* mutants displayed an erythropoietin (Epo)-dependent polycythemia in heterozygotes and a hypochromic, microcytic anemia in homozygotes. Interestingly, both defects in erythropoiesis were transient, correcting by young adulthood. Delayed upregulation of the negative hormonal regulator of iron homeostasis, hepcidin (*Hamp*), during postnatal development correlates strongly with profound increases in Fpn1 protein levels and polycythemia in *Pcm* heterozygotes. Thus, our data suggest that a *Hamp*-mediated regulatory interference alleviates the defects in iron homeostasis and transient alterations in erythropoiesis caused by a regulatory mutation in *Fpn1*.

Key words: Ferroportin 1, Iron homeostasis, Hepcidin

Introduction

Iron is an essential element, necessary for the synthesis and activity of both heme and non-heme proteins and enzymes. However, iron levels must be carefully controlled organismally, as cellular damage can result from its untoward oxidation-reduction chemistry (for a review, see Aisen et al., 2001). Owing to lack of efficient means of excretion, iron homeostasis is principally regulated at the level of organismal uptake by the duodenal enterocyte. Regulation occurs at both the apical and basolateral membranes to effect transcellular movement of iron from the gut lumen to the portal circulation (for a review, see Roy and Enns, 2000). At the apical surface, ferrous iron is transported into the enterocyte via the proton symporter DMT1 (for a review, see Andrews, 1999). Recently, ferroportin 1 (Fpn1; also known as MTP1, IREG1, SLC11A3; SLC40A1 – Mouse Genome Informatics) has been identified as the basolateral iron transporter of the duodenal enterocyte (Abboud and Haile, 2000; Donovan et al., 2000; McKie et al., 2000). Cellular export of iron and loading onto serum transferrin requires ferroxidase activity, served by the multicopper oxidase hephaestin (Vulpe et al., 1999) in the duodenal enterocyte, and by its homologue ceruloplasmin (for a review, see Hellman and Gitlin, 2002) in other cells types. From the portal circulation, transferrin-bound iron is taken up by liver cells via the transferrin (Tf)-transferrin receptor (TfR) system, the principal mechanism of iron delivery to iron-using cells (for a review, see Richardson and Ponka, 1997).

Although steady-state iron levels are maintained by enteral absorption of iron (for a review, see Finch, 1994), the majority of iron used for cellular requirements derives from iron recycled by the reticuloendothelial macrophage system (for a review, see Knutson and Wessling-Resnick, 2003). Fpn1 has been implicated in turnover of iron recovered from scavenged red blood cells in reticuloendothelial macrophages of the splenic red pulp and hepatic Kupffer cells (Abboud and Haile, 2000; Yang et al., 2002). The essential role of Fpn1 in iron homeostasis has been revealed by mutations in human FPN1, leading to autosomal dominant iron overload in reticuloendothelial macrophages (Montosi et al., 2001; Njajou et al., 2001; Cazzola et al., 2002; Devalia et al., 2002; Arden et al., 2003; Rivard et al., 2003; Jouanolle et al., 2003). This unique pattern of iron accumulation caused by a mutation in *FPN1*, comprising type IV hereditary hemochromatosis, contrasts distinctly to the primarily parenchymal accumulation seen in the more common, recessively inherited HFE-associated hemochromatosis (type I) (for a review, see Ajioka and Kushner, 2002). All known mutations in *FPN1* map to the

coding region, and both gain- and loss-of-function mechanisms have been evoked in disease pathogenesis (for a review, see Fleming and Sly, 2001).

The post-transcriptional regulation of iron-relevant proteins, including TfR and ferritin, is achieved by the interaction of iron regulatory proteins (IRPs) with iron responsive elements (IREs) located within the untranslated regions (UTR) of the mRNA (for a review, see Aisen et al., 2001). In the case of ferritin, an IRE sequence in the 5′ UTR forms a secondary, stem-loop structure that is bound by iron regulatory protein 1 (IRP1) in the absence of intracellular iron, inhibiting protein translation (for a review, see Hentze and Kuhn, 1996). Likewise, *Fpn1* transcripts contain an IRE sequence in the 5′ UTR, which inhibits translational efficiency of *Fpn1* mRNA in the absence of intracellular iron in cell culture (Abboud and Haile, 2000; McKie et al., 2000; Liu et al., 2002). Here, positional cloning of the *Pcm* mutation identified a hypermorphic allele of *Fpn1* which, in the absence of an IRE in the 5′UTR, affects its translational regulation, leading to increased Fpn1 protein levels during early postnatal development despite low cellular iron levels.

Dietary absorption of iron responds to body iron levels via a putative regulator, conveying organismal iron status to remote effectors of iron balance (for a review, see Finch, 1994). The expression of the hepcidin antimicrobial peptide (Hamp; also known as Hepc, LEAP-1), a disulfide-bridged oligopeptide produced in the liver (Park et al., 2001), is responsive to body iron stores (Pigeon et al., 2001). Severe dysregulation of iron balance in murine models of *Hamp* gain- and loss-of-function (Nicolas et al., 2001; Nicolas et al., 2002a), as well as failure of *Hamp* induction in a murine model for HFE hemochromatosis (Ahmad et al., 2002; Nicolas et al., 2003) reveal Hamp as the principal hormonal regulator of iron homeostasis. Furthermore, mutations in human *HAMP* lead to a severe, juvenile form of hereditary hemochromatosis (type II) (Roetto et al., 2003).

In the present study, downregulated expression of *Hamp* correlated with high levels of Fpn1 protein expression and polycythemia in *Pcm* mutant animals. Developmental analysis of *Hamp* expression indicates an interference on *Fpn1* regulation that is superimposed on the primary defects caused by the microdeletion in the *Fpn1* promoter region, and alleviates the abnormalities in iron homeostasis and erythropoiesis in *Pcm* mutant animals. Our results provide the most compelling evidence to date implicating Hamp in the systemic regulation of Fpn1 expression in vivo.

Materials and methods

Mice and genotyping

Pcm mice were generated by radiation mutagenesis of (101/HeH×C3H/HeH) F1 hybrids (Cattanach, 1995). The present study involved partial congenics on an A/J background; most analyses were performed on animals from N5 and subsequent backcross generations. A genome scan to determine the chromosomal location of *Pcm* by residual heterozygosity mapping employed N3 and N4 backcross animals at 7 weeks of age. Twenty-one wild type and 13 mutants showing hematocrit (Hct) greater than 50% were genotyped by PCR using a simple sequence length polymorphism (SSLP) marker panel consisting of 81 markers (Research Genetics) polymorphic among A/J and the parental strains. Markers displayed an average spacing of 15-20 cM. Marker and genome scan information are available from authors upon request. All animal experiments in this study were approved by the Institutional Animal Care and Use Committee of Baylor College of Medicine.

Red blood cell analyses

Hematocrit measurements, expressed as a percentage, were obtained by standard microcapillary determination. Determination of mean corpuscular volume (MCV), and mean corpuscular hemoglobin content (MCHC) was performed on the ADVIA 120 Hematology System (Bayer). Blood was collected in EDTA-coated collection tubes (Sarstedt) at postnatal day 0 (P0) and 12 weeks of age for analysis.

Serum and tissue iron determination

Quantification of iron concentration was performed based on methodology of Torrance and Bothwell (Torrance and Bothwell, 1980). Equal volumes of 0.2 N HCl with 0.05% ascorbic acid, and 11% trichloroacetic acid were added to serum samples. Tissue samples were digested in 3 N HCl with 10% trichloroacetic acid at 65°C overnight. Colorimetric iron determination of supernatants was performed using the Total Iron Measurement Kit (Sigma).

In vitro bone marrow cultures

Erythroid lineage terminal differentiation as a readout for erythroid-committed precursor and progenitor cell abundance in the bone marrow was determined by a fluorescence-activated cell sorting (FACS)-based approach to quantify erythropoietin (Epo)-dependent expression of erythroid lineage marker TER-119, expressed in mature erythrocytes. Bone marrow cells were flushed from dissected femurs, washed and lysed of erythrocytes in buffer containing 155 mM NH_4Cl, 10 mM NH_4HCO_3 and 0.1 mM EDTA pH 8.0. As determined by Coulter Z2 particle counter, 1×10^6 cells were plated in Iscove's Modified Dulbecco's Medium (Invitrogen) containing 30% FBS (Stem Cell) in 1 ml. Parallel cultures were set up with and without recombinant human Epo (Amgen) at a final concentration of 3000 mU/ml. Cells were cultured in a humidified incubator at 37°C and 5% CO_2. To determine the percentage of TER-119-expressing cells, uncultured cells (day 0) and cells on day 2 were harvested, and washed in PBS. Cells were incubated with biotinylated antibody against mouse TER-119 (BD Pharmingen) for 30 minutes on ice at 1:100 dilution. After washing, cells were incubated with streptavidin-phycoerythrin (BD Pharmingen) for 10 minutes at 1:50 dilution, washed and resuspended in PBS. The percentage of TER-119-expressing cells was determined by flow cytometry using the Coulter Epics XL-MCL.

Histology

Liver and spleen samples were dissected, fixed in Bouin's reagent, dehydrated in a graded series of ethanol, embedded in paraffin wax and sectioned at 5-10 μm. To determine the abundance and localization of iron, Prussian Blue staining was performed using the Accustain iron staining kit (Sigma), and photographed using light microscopy. Femurs from mice were dissected, cleaned and fixed in a 1:1 solution of 37% formaldehyde and B-5 fixative stock solution (Poly Scientific). After light decalcification, femurs were paraffin wax embedded and sectioned. To assess the relative abundance of hemoglobinized cells in the bone marrow, paraffin wax-embedded femoral sections were rehydrated, fixed for 10 minutes in methanol, and subjected to *o*-dianidisine (O-D) staining. Slides were incubated for 10 minutes in O-D working solution containing 5 volumes of 0.2% O-D in methanol, 1 volume of 1% sodium nitroprusside in water and 1 volume of 3% hydrogen peroxide.

RACE and RT-PCR

Total RNA from liver and kidney tissue samples was isolated using TRIzol Reagent (Invitrogen). The 5′ ends of *Fpn1* transcripts in wild-type and homozygous mutant animals were determined by rapid

amplification of cDNA ends (RACE) using the SMART RACE cDNA amplification kit (Clontech) on 1 μg total RNA derived from livers of 3-week-old mice. RACE PCR was achieved using a gene-specific primer in *Fpn1* corresponding to sequence 5′-ATGACGGACA-CATTCTGAACCA-3′. RT-PCR to determine approximate level of transcript abundance for *Fpn1* and *Hamp* was performed on total RNA derived from livers of 7-week-old animals. First-stand cDNA was synthesized from 2 μg total RNA using standard methods. PCR amplification conditions consisted of 25 cycles: denaturation at 94°C for 30 seconds, annealing at 56°C for 30 seconds, and extension at 72°C for 30 seconds. Primer sequences for *Fpn1* are 5′-ACA-AACAAGGGGAGAACGC-3′ (forward) and 5′-ATGACGGACAC-ATTCTGAACCA-3′ (reverse); published primer sequences for *Hamp* (*Hepc1*) and β-actin were used (Nicolas et al., 2001).

Quantitative real-time RT-PCR

Epo and *Fpn1* mRNA expression were quantified via real-time RT-PCR on total RNA samples isolated from liver and kidney from 3-week-old animals and kidney from 12-week-old animals. Reactions and signal detection were performed on an ABI Prism 7000 Sequence Detection System (Applied Biosystems). *Epo* primers [5′-TCAA-CTTCTATGCTTGGAAAAGAATG-3′ (forward), 5′-TGAGAGAC-AGCGTCAAGATGAGA-3′ (reverse)] and TaqMan MGB probe (5′-CGCTAGCGACCTGGA-3′) were labeled with 6-FAM (Applied Biosystems). *Fpn1* primer sequences [5′-GGGTGGATAAGAA-TGCCAGACT-3′ (forward) and 5′-ATGACGGACACATTCTGAA-CCA-3′ (reverse)] were assayed via SYBR Green fluorescence detection. *18S* rRNA assay was performed using primers 5′-TCGAGGCCCTGTAATTGGAA-3′ (forward), 5′-CCCTCCAATGG-ATCCTCGTT-3′ (reverse); and TaqMan MGB probe 5′-AGT-CCACTTTAAATCCTT-3′ was labeled with 6-FAM (Applied Biosystems). Relative amounts of mRNA are expressed as a ratio to *18S* rRNA expression, and normalized to a single wild-type ratio arbitrarily set to 1.

Western analysis of liver and duodenum

For western blot analyses, liver and duodenal samples were collected, homogenized and lysed in RIPA buffer plus Complete®, EDTA-free protease inhibitor (Roche). Extract supernatant was collected and protein quantified using the BioRad *DC* Protein Assay kit (BioRad). The samples were mixed with equal volume sample buffer with β-mercaptoethanol. Unboiled samples were used for Fpn1 and actin detection, boiled samples for ferritin; 10 μg total protein from liver lysates and 5 μg from duodenum were loaded per lane. Samples were separated using 8 or 10% SDS-PAGE and transferred to PVDF membrane. Blocking was achieved by incubation in TRIS-buffered saline containing 5% BSA and 0.1% Tween 20. Membranes were incubated overnight at 4°C using primary antibodies against mouse Fpn1 (kindly provided by M. Hentze) at 1:2000, horse ferritin from spleen (Sigma) at 1:5000, or mouse actin (Santa Cruz) at 1:5000. After washing, membranes were incubated with horseradish peroxidase-conjugated secondary antibodies (1:5000) against rabbit (for Fpn1 and ferritin) or goat (for actin), and signal developed using ECL reagent (Santa Cruz Biotechnology).

Statistical analyses

All data are reported as the mean±s.d. All comparisons were made versus wild-type cohorts, and analyzed for significant differences using the Student's unpaired *t*-test.

Results

Aberrant hematocrit in *Pcm* mutant mice

The *Pcm* mutation was generated by X-irradiation of (101/HeH×C3H/HeH) F1 hybrid animals, and identified by increased redness of the ears and feet of adult progeny (Cattanach, 1995). Mutant heterozygous animals exhibited an incompletely penetrant increase in Hct up to 75% in young adult animals. Our analysis of the *Pcm* mutation on a partially congenic A/J background reiterated the preliminary report on the increased redness in the ear and footpad vasculature of heterozygous mutant animals (Cattanach, 1995), most highly expressed around 7 weeks of age (Fig. 1A). Consistent with the external phenotype, Hct analysis of heterozygous mutant animals demonstrated a highly penetrant polycythemia at 7 weeks of age when compared with wild-type littermates (*Pcm*/+ Hct 69.1±12.0% versus +/+ Hct 44.3±3.6%; $P<0.001$) (Fig. 1B). The polycythemia in heterozygous mutants was transient in nature, as the Hct corrected to baseline by 12 weeks of age. Strikingly, homozygous mutants were remarkable for a congenital anemia at postnatal day 0 (P0) (*Pcm/Pcm* Hct 22.4±5.3% versus +/+ Hct 44.8±9.4%; $P<0.001$). The homozygous mutants corrected for the significant perinatal anemia by 7 weeks of age, and were indistinguishable from wild-type and heterozygous Hct levels by 12 weeks of age (Fig.

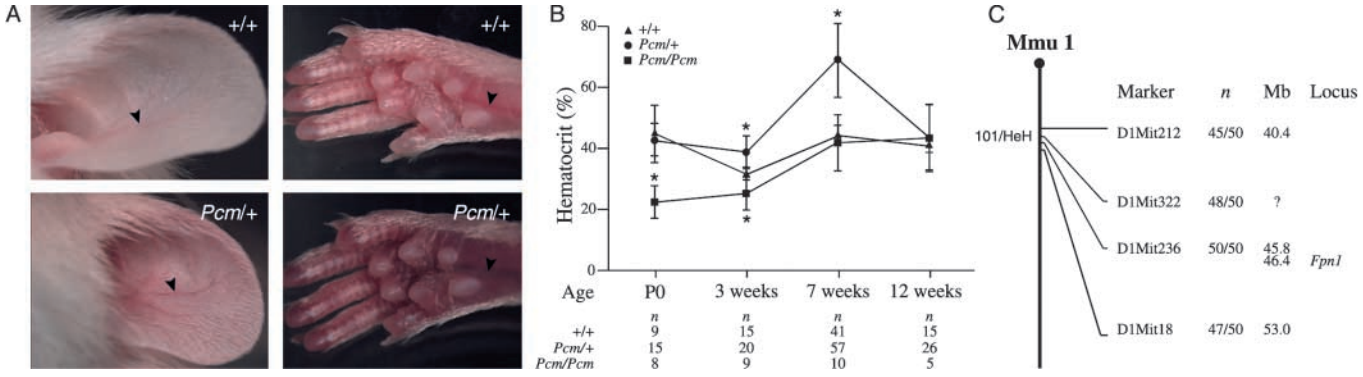

Fig. 1. *Pcm* heterozygotes are characterized by external ruddiness and transient polycythemia mapping to proximal chromosome 1. (A) Ears and hindpaws show increased redness in 7-week-old heterozygous mice, particularly in vasculature (arrowheads). (B) Microcapillary hematocrits measured at several postnatal timepoints demonstrate transient polycythemia in *Pcm/+* mice, and a transient anemia in *Pcm/Pcm* mice. Asterisk, $P<0.001$ for mutant classes when compared with wild-type mice per timepoint. (C) *Pcm* critical region. Phenotype co-segregates with microsatellite marker D1Mit236; *n* represents ratio of *Pcm/+* mutant progeny (Hct > 55%) retaining heterozygosity for parental alleles (101/HeH) of markers. Physical map position (Mb) as per the Sanger Centre mouse genome assembly (NCBI Build 30).

1B). Additionally, there was no evidence for involvement of non-erythroid hematopoietic cell lineages in polycythemic mutant animals (data not shown). Wild-type animals were remarkable for a nadir in Hct at 3 weeks of age, consistent with the physiological anemia observed in young mice (Bechensteen and Halvorsen, 1996).

Chromosomal localization of the *Pcm* locus

We mapped the *Pcm* mutation to a subchromosomal region by using a genome-wide panel of SSLP markers to detect heterozygosity in partially congenic lines. Using elevation of Hct at 7 weeks of age to define heterozygous mutants, only a single marker, D1Mit236, retained residual heterozygosity for the parental SSLP allele in 100% of mutants screened (Fig. 1C). Thus, the *Pcm* mutation segregated as a single-gene trait. The informative markers delineated a 6 cM critical region on chromosome 1 (Mmu 1), which does not encompass any known polycythemia-associated loci. No sizeable genomic deletions were detected in any of over 50 genes and loci located within and near the 6 cM critical region, as determined by PCR amplification of genomic DNA from *Pcm* animals homozygous at D1Mit236 (data not shown).

A 58 bp microdeletion in the *Fpn1* promoter represents the *Pcm* mutation

Severe embryonic anemia has been reported for a loss-of-function allele of the zebrafish homologue of *Fpn1* (Donovan et al., 2000), an evolutionarily highly conserved iron transporter mapping to within 1 Mb of D1Mit236 (Fig. 1B). Given the presence of severe perinatal anemia in *Pcm* homozygous animals, *Fpn1* represented the strongest candidate gene for *Pcm*. However, in contrast to mutant human (Montosi et al., 2001; Njajou et al., 2001; Cazzola et al., 2002; Devalia et al., 2002; Arden et al., 2003; Jouanolle et al., 2003; Rivard et al., 2003) and zebrafish (Donovan et al., 2000) alleles, we detected no coding region mutations in *Fpn1*. Instead, a 58 bp microdeletion was detected immediately upstream to the transcription start site, in close proximity to putative promoter elements, such as a TATA box (Fig. 2A). The microdeletion, comparable in size to other radiation-induced lesions (Grosovsky et al., 1988; Miles and Meuth, 1989), was absent in the parental strains and co-segregated invariably with the mutant phenotype (Fig. 2B).

The 58 bp deletion leads to lack of IRE in *Fpn1* mRNA

Using 5′RACE to assess *Fpn1* transcript identity, we observed a single band from wild type, but multiple smaller PCR products from *Pcm/Pcm* samples (Fig. 2C). A consistent amplification pattern was observed in all three homozygous samples tested. DNA sequence analysis of 5′RACE products from wild-type animals reiterated recent data demonstrating *Fpn1* transcription start site proximity to the TATA box (Liu et al., 2002). Importantly, mutant RACE products revealed multiple transcription start sites, both upstream and downstream of the wild-type start site. For example, in a subset of transcripts, initiation occurred 845 bp upstream of the wild-type transcription start site, followed by splicing downstream of the IRE, with no evidence of in-frame, upstream translation initiation sequences (Fig. 2A). Other transcripts initiated downstream of the IRE, but upstream of the translation initiation codon, retaining the wild-type open reading frame. In total, only one of 10 cDNAs retained the IRE present in the *Fpn1* wild-type 5′UTR (Fig. 2A) (Abboud and Haile, 2000; Donovan et al., 2000; McKie et al., 2000). Importantly, mutant transcript abundance was not affected (Fig. 2D).

Abnormal iron balance in *Pcm* mice

Several mouse models of defective iron balance are characterized by a severe, congenital anemia (Bannerman et al., 1973; Bernstein, 1987; Nicolas et al., 2002a). Indeed, peripheral blood smears from anemic, *Pcm/Pcm* mice were remarkable for hypochromic, microcytic erythrocytes at P0 (Fig. 3A). Additionally, quantitative analysis of red cell indices at P0 demonstrated significantly lowered MCV [*Pcm/Pcm* MCV 75.2±2.7 fl (n=10), versus +/+ MCV 104±6.4 fl (n=6); P<0.0001] and MCHC [*Pcm/Pcm* MCHC 21.2±4.1 g/dl (n=10), versus +/+ MCHC 29.3±3.3 g/dl (n=6); P<0.01] in homozygous mutants. Furthermore, whereas P0 wild-type hepatocytes contained significant iron stores, *Pcm/Pcm* hepatocytes were devoid of stainable iron (Fig. 3B). Quantification of organismal iron levels at P0 showed that

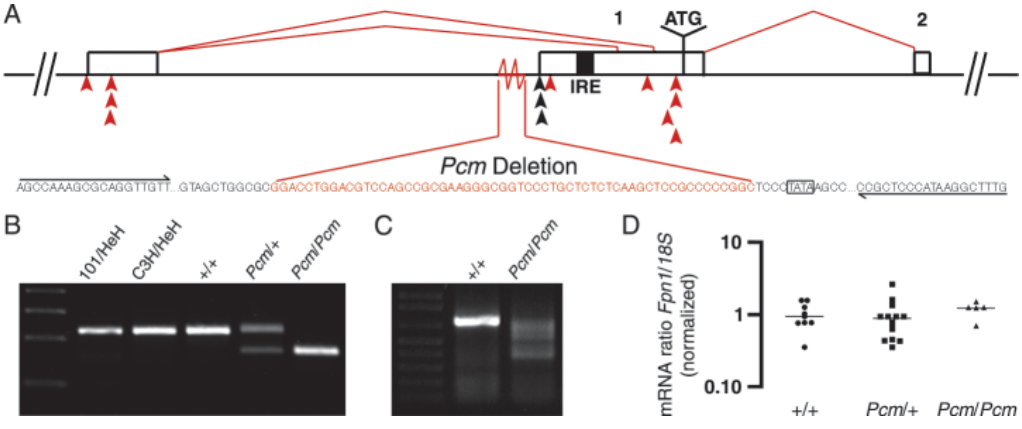

Fig. 2. Deletion in promoter region of *Fpn1* leads to altered transcriptional initiation, but not transcript abundance, in *Pcm* mutant mice. (A) A 58 bp deletion in the promoter region of *Fpn1* constitutes the *Pcm* mutation. Black arrowheads indicate wild-type transcription initiation site determined by 5′RACE, red arrowheads indicate *Pcm*/*Pcm* initiation sites. ATG, translational start; IRE, iron responsive element; boxed region indicates TATA box. (B) Mutant phenotype co-segregates with deletion in *Fpn1*, as demonstrated by PCR genotyping using primers indicated by overlined and underlined sequences in A. Wild-type band 230 bp; mutant band 172 bp. (C) 5′RACE PCR demonstrates altered *Fpn1* transcript identity in *Pcm* mutant mice. Wild-type band 630 bp. (D) Real-time RT-PCR to quantify *Fpn1* transcript abundance reveals no statistically significant difference among genotypes at 3 weeks of age. The horizontal line indicates the median.

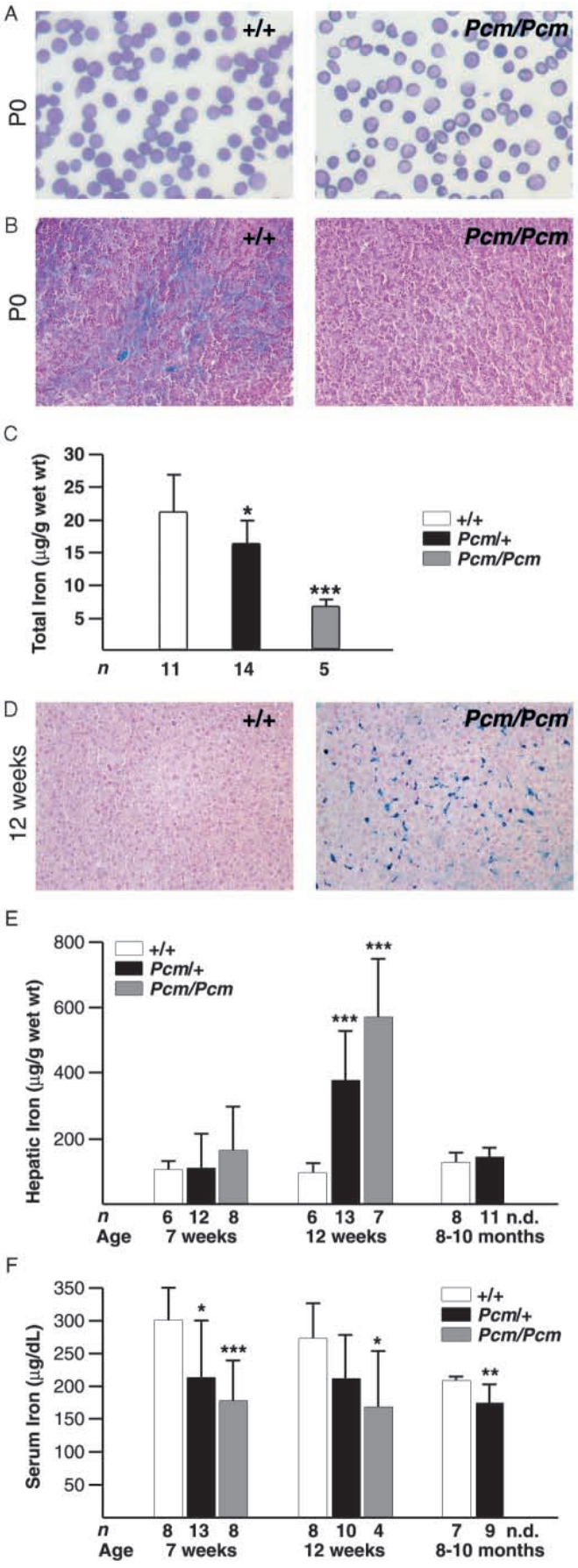

Fig. 3. Iron deficiency anemia at birth and iron accumulation in young adults in *Pcm* mutant mice. (A) Peripheral blood smear remarkable for hypochromic, microcytic red blood cells in *Pcm/Pcm* mice at P0. Wright-Giemsa stain. (B) Prussian Blue staining of P0 liver sections reveals decreased parenchymal liver iron in *Pcm/Pcm* mice. (C) Quantification of total iron at P0 demonstrates organismal iron deficiency in *Pcm* mutant pups. (D) Prussian Blue staining of sections of 12-week-old liver shows numerous localized iron deposits in *Pcm/Pcm* mice. (E) Hepatic iron content significantly elevated by 12 weeks of age in *Pcm*/*Pcm* mice. (F) Decreased serum iron levels in *Pcm* mutants compared with wild type. Asterisk, $P<0.05$; double asterisk, $P<0.01$; triple asterisk, $P<0.001$.

mutant pups were iron-deficient, most severely in homozygous mutants (Fig. 3C). Strikingly, the perinatal iron deficiency progressively reversed to an iron overload phenotype during postnatal development, resulting in a predominantly localized hepatic iron accumulation reminiscent of a reticuloendothelial macrophage distribution pattern at 12 weeks of age (Fig. 3D) (Yang et al., 2002). By contrast, no iron accumulation was observed in livers from wild-type littermates (Fig. 3D). Quantification of hepatic iron demonstrated a significant, graded elevation in iron levels at 12 weeks of age, highest in *Pcm* homozygous mutant animals (Fig. 3E). Both at P0 and 12 weeks of age, heterozygous animals exhibited intermediate levels of hepatic iron staining (data not shown), consistent with tissue iron quantification (Fig. 3C,E). Decreased serum iron in *Pcm* mutant animals at 7 and 12 weeks of age in the context of hepatic iron accumulation (Fig. 3D,E) is consistent with increased tissue iron sequestration and/or use during erythropoiesis (Fig. 3F).

Transient alterations in Epo-dependent erythropoiesis in *Pcm* mice

To assess the role of Epo signaling in mutant animals, we measured *Epo* transcript levels via real-time RT-PCR analysis. We observed significantly elevated *Epo* transcript abundance in 3-week mutant animals from both the kidney, the primary site of Epo production, and the liver, an important auxiliary site particularly during stress erythropoiesis (Fig. 4A) (Bonderant and Koury, 1986). Additionally, we measured erythroid differentiation of bone marrow cells cultured in the presence or absence of Epo by determining TER-119 positivity at day 2, which reflects differentiation of cells at the CFU-E stage and beyond (Kina et al., 2000). Recently, similar in vitro culture methods have been shown to closely approximate in vivo differentiation of erythroid progenitors (Zhang et al., 2003). Homozygous mutant bone marrow demonstrated significantly increased erythroid differentiation in the presence of Epo at 3 weeks of age (Fig. 4B), consistent with normalization of the P0 anemia by early adulthood (Fig. 1B). At 7 weeks of age, *o*-dianidisine staining for hemoglobinized cells in heterozygous bone marrow sections demonstrated hypercellularity and increased abundance of erythrogenic foci (Fig. 4C). Additionally, heterozygous bone marrow showed significantly elevated erythroid differentiation in vitro (Fig. 4D), in agreement with marrow-derived red cell production leading to polycythemia. By 12 weeks of age, consistent with the resolution of the transient alterations in hematocrit observed in both heterozygous and homozygous mutant animals (Fig. 1C), no statistically significant differences in kidney *Epo* transcript

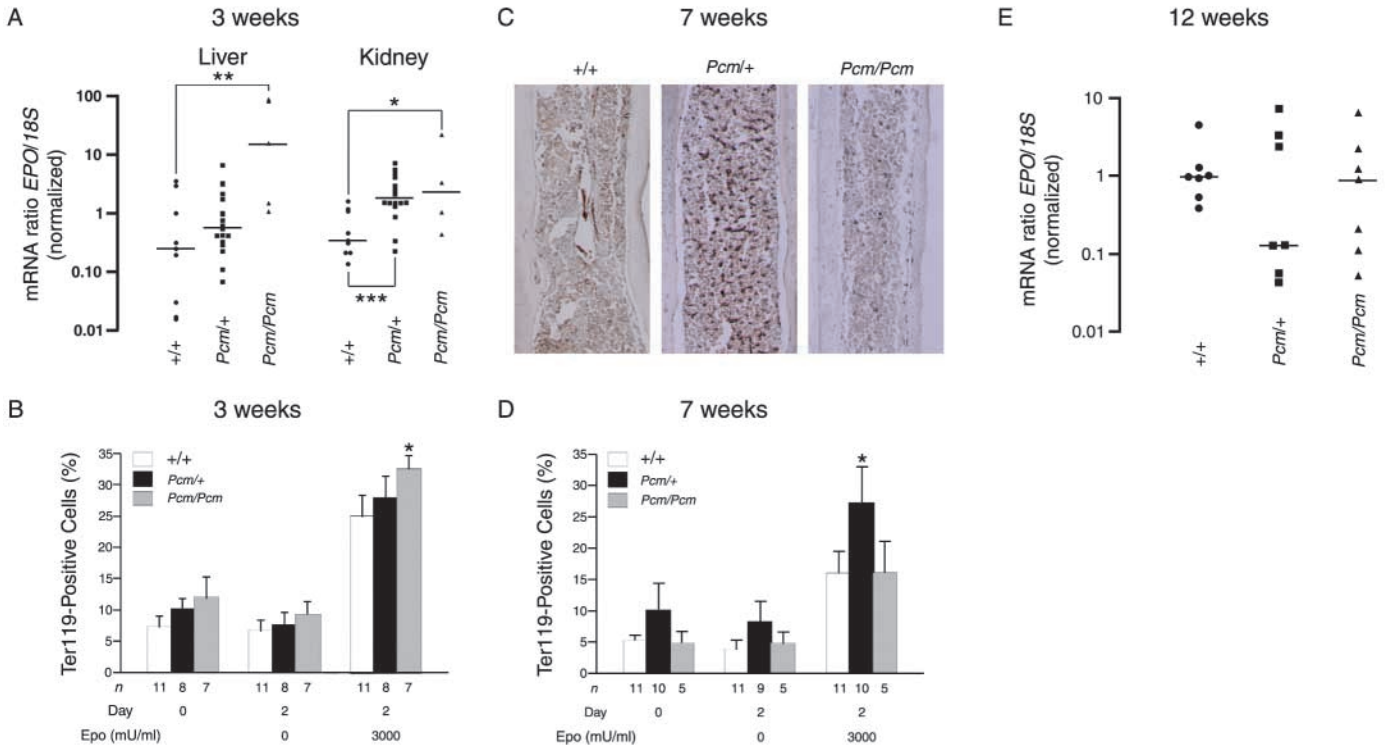

Fig. 4. Polycythemia is secondary to Epo-driven, bone marrow-derived red cell production. (A) Real-time RT-PCR reveals elevated *Epo* transcript levels in mutant liver and kidney at 3 weeks of age. The horizontal line indicates the median. **P*<0.05; ***P*<0.01; ****P*<0.001. (B) In vitro, FACS-based determination of late-progenitor and precursor erythroid cell differentiation to Ter119-positivity. *Pcm/Pcm* mice at 3 weeks of age show increased bone marrow erythroid activity at day 2. **P*<0.001. (C) Increased hemoglobinization and cellularity of *Pcm/+* bone marrow, as demonstrated by O-D staining of sections at 7 weeks of age. (D) In vitro analysis reveals increased bone marrow erythroid activity in *Pcm/+* mice at 7 weeks of age. **P*<0.001. (E) Real-time RT-PCR using 12-week kidney samples shows no statistically significant differences in *Epo* transcript levels among genotypes. The horizontal line indicates the median.

levels were detected (Fig. 4E). Additionally, the microcytosis observed at P0 (Fig. 3A) reversed to moderately elevated MCV at 12 weeks of age in both heterozygotes [*Pcm*/+ MCV 44.8±1.2 fl (*n*=10), versus +/+ MCV 42.4±0.7 fl (*n*=4); *P*<0.01] and homozygotes [*Pcm/Pcm* MCV 46.7±2.3 fl (*n*=6); *P*<0.01], whereas no statistically significant differences in MCHC were observed (data not shown), indicating resolution of hypochromia.

Lack of the IRE in *Fpn1* mRNA confers profound elevations in Fpn1 protein levels during early postnatal development

As the IRE inhibits translational efficiency of *Fpn1* mRNA in the absence of intracellular iron (Abboud and Haile, 2000; McKie et al., 2000; Liu et al., 2002), aberrant *Pcm* mRNAs lacking an IRE are likely not to be repressed by low cellular iron states. Indeed, western analysis demonstrated a graded increase in hepatic Fpn1 expression at P0, with a several-fold increase in Fpn1 levels in mutant livers, highest in homozygotes (Fig. 5A). By contrast, the expression level of ferritin, which directly correlates with intracellular iron content via IRE-dependent post-transcriptional regulation (Hentze et al., 1987) (for a review, see Aisen et al., 2001), showed the expected graded decrease in mutant livers, lowest in homozygotes (Fig. 5A). These results were consistent with decreased hepatic iron staining and organismal iron levels at P0 (Fig. 3B,C). Similarly, a graded increase in hepatic Fpn1 protein expression was seen in 3-week-old mutants (Fig. 5B), whereas low levels of ferritin expression correlated with a lack of hepatic iron staining in all genotypes at this stage (data not shown). Thus, in the absence of an IRE, *Pcm* mutant *Fpn1* transcripts are not subject to iron/IRE-mediated translational regulation. This is manifested as increased hepatic Fpn1 protein expression during early postnatal life, representing the direct effect of the *Pcm* microdeletion in *Fpn1*. Based on the increased Fpn1 protein levels and absence of aberrant Fpn1 isoforms by western analysis (data not shown), *Pcm* is considered a hypermorphic allele of *Fpn1*.

Elevated Fpn1 expression correlates with polycythemia in young adult mice

At 7 weeks, wild-type Fpn1 protein expression was low (Fig. 5C), consistent with a decreased demand for iron as organismal growth rate declines. Interestingly, elevated Fpn1 protein expression was observed exclusively in polycythemic mutant animals. An identical expression pattern was observed in the duodenum (Fig. 5D). This probably excludes tissue-specific regulatory mechanisms, which have been proposed to confer reciprocal regulation of Fpn1 expression in the liver and duodenum (Abboud and Haile, 2000). Although the majority of heterozygous mutant mice were polycythemic at 7 weeks of age, a subset of animals (12.3%) displayed reduced phenotypic expressivity with Hcts of less than 50%. Therefore, we determined whether Fpn1 protein levels correlated with

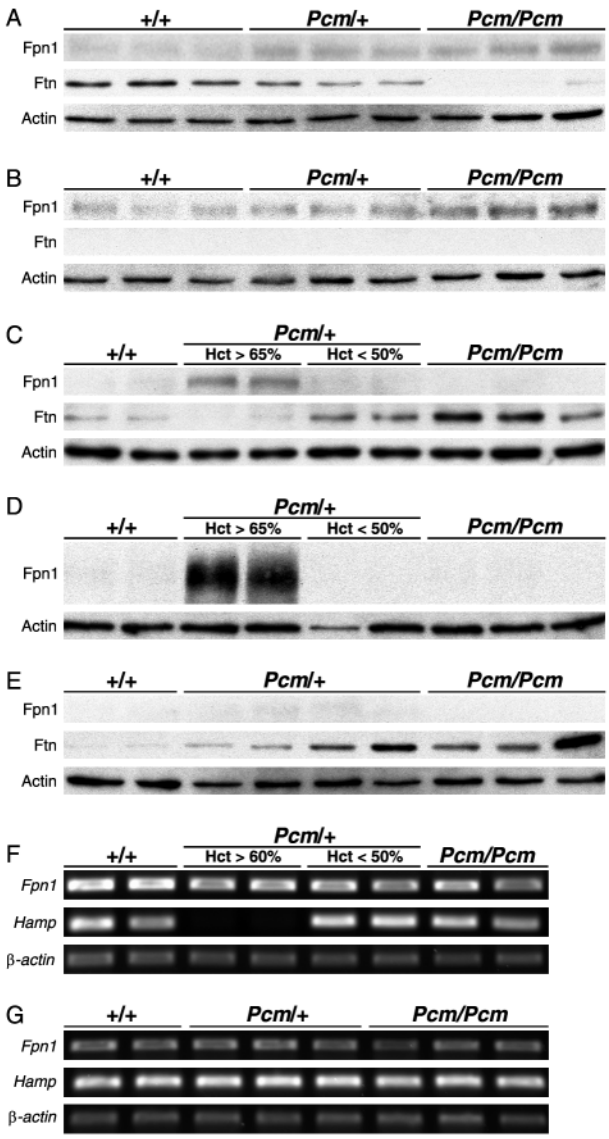

Fig. 5. Altered Fpn1 protein and *Hamp* mRNA expression in *Pcm* mutant mice. (A) Western blot analysis reveals graded increase in Fpn1 protein expression in P0 mutant liver, with concomitant graded decrease in ferritin expression. Approximate molecular masses: Fpn1, 68 kDa; ferritin (Ftn), 20 kDa; actin, 41 kDa. (B) Three-week-old liver shows similar graded increase in Fpn1 protein expression on a western blot. (C) Seven-week-old liver exhibits persistence of Fpn1 protein expression only in polycythemic *Pcm* heterozygous mice on a western blot. (D) Seven-week-old duodenum demonstrates pattern of Fpn1 protein expression similar to liver on a western blot. (E) Twelve-week-old liver reveals downregulation of Fpn1 protein expression in all genotypes on a western blot. (F) Seven-week-old liver RT-PCR shows no significant difference in *Fpn1* mRNA expression, but lack of *Hamp* mRNA expression in polycythemic mutant mice. Band sizes: *Fpn1*, 338 bp; *Hamp*, 171 bp; β-*actin*, 250 bp. (G) Twelve-week-old liver RT-PCR demonstrates upregulation of *Hamp* mRNA expression in all animals.

either Hct subgroup. Indeed, in contrast to polycythemic heterozygotes, non-polycythemic heterozygotes and homozygotes demonstrated baseline Fpn1 expression (Fig. 5C,D). Thus, elevated duodenal and hepatic Fpn1 levels are likely to be permissive for the polycythemia at 7 weeks, regulating increased duodenal iron uptake and decreased cellular iron storage and sequestration. As *Fpn1* transcript abundance was unaffected (Fig. 5F), the profound increase in Fpn1 protein levels at 7 weeks of age results from a predominantly post-transcriptional, rather than transcriptional, mechanism of Fpn1 regulation. Furthermore, this regulatory effect appears to be superimposed on the primary defect caused by the microdeletion in the *Fpn1* promoter region, i.e. a moderate, graded increase in Fpn1 expression because of the absence of the IRE (Fig. 5A,B). By 12 weeks of age, Fpn1 protein levels were downregulated in all genotypes, whereas increased ferritin expression in mutants reflected increased hepatic iron localization (Fig. 5E), confirming hepatic iron accumulation (Fig. 3D,E).

Delayed upregulation of *Hamp* in polycythemic mutant mice at 7 weeks of age

Recent studies in mice and individuals with juvenile hemochromatosis have implicated Hamp as the hormonal regulator of iron homeostasis (Nicolas et al., 2001; Park et al., 2001; Pigeon et al., 2001; Nicolas et al., 2002a; Ahmad et al., 2002; Nicolas et al., 2003; Roetto et al., 2003). *Hamp* is expressed at very low levels during most of embryonic and early postnatal development, and displays significant upregulation by P56 (Nicolas et al., 2002a). Strikingly, at 7 weeks of age, low levels of *Hamp* expression were restricted to polycythemic *Pcm* mutant mice, whereas upregulation of *Hamp* correlated with normal Hct (Fig. 5F). By 12 weeks of age, *Hamp* expression was upregulated in all animals (Fig. 5G), correlating with normalization of Hct in both mutant genotypes as well as downregulation of Fpn1 protein expression (Fig. 5E). Western analysis for Fpn1 and RT-PCR for *Hamp* were representative: of the high Hct mutants tested (Hct>60%), 12 of 13 animals showed high Fpn1 protein levels, while 11 of 13 animals expressed low *Hamp* mRNA levels. Conversely, in the low Hct cohort (Hct<50%), all animals tested (n=8) displayed both downregulated Fpn1 protein levels and upregulated *Hamp* expression. All wild-type samples (n=6) exhibited low Fpn1 protein and upregulated *Hamp* transcript levels.

Normalization of hepatic iron accumulation in aged mutant animals

Downregulation of Fpn1 protein levels in *Pcm* mutant animals at 12 weeks of age (Fig. 5E) would be predicted to abrogate organismal iron uptake due to Fpn1-mediated duodenal iron absorption, eventually normalizing iron levels with time. In fact, an aged cohort of heterozygous mutant animals demonstrated normalization of hepatic iron levels by 8-10 months of age (Fig. 3E). This correlated with greatly decreased hepatic iron staining, characterized by residual reticuloendothelial localization (data not shown). Interestingly, heterozygous mutant serum iron levels at this time point were lowered significantly versus wild type (Fig. 3F), consistent with tissue iron sequestration resulting from Hamp regulation. Additionally, *Pcm*/+ mutants were anemic [*Pcm*/+ Hct 36.8±2.4% (n=8), versus +/+ Hct 42.9±2.5% (n=11); P<0.0001]. Thus, low serum iron levels and sequestration of iron in reticuloendothelial stores are reminiscent of the anemia of chronic disease (for a review, see Means, 2003), and appear to be the disease endpoint in *Pcm* mutant animals.

Discussion

Positional cloning of the *Pcm* mutation reveals a microdeletion in the *Fpn1* promoter region causing disruption of iron balance and erythropoiesis in *Pcm* mutant animals. Elevated Fpn1 protein expression during early postnatal life in *Pcm* mutant animals represents the direct mutational effect of IRE ablation because of aberrant transcriptional start sites. Although previous studies have shown that the *Fpn1* IRE regulates protein expression in a post-transcriptional manner in vitro (Abboud and Haile, 2000; McKie et al., 2000; Liu et al., 2002), to our knowledge, this is the first report demonstrating the in vivo role for the *Fpn1* IRE. Indeed, there is precedence for IRE-based mutations causing human disease. The initial mutation identified in hereditary hyperferritinemia-cataract syndrome involved a point mutation in the IRE located in the 5′UTR of L-ferritin (Girelli et al., 1995). Subsequently, numerous mutations have been identified within the L-ferritin IRE, including a 29 bp deletion predicted to abolish IRE-mediated regulation of protein translation (Girelli et al., 1997). To date, no mutations affecting IRE function have been identified in the *FPN1* locus. Our results suggest that regulatory mutations may comprise a novel subset of *FPN1* alleles, and should be suspected when features of type IV hemochromatosis are present in the absence of coding region mutations.

Changes in iron homeostasis induced by acute inflammatory stimuli require *Hamp* upregulation (Nicolas et al., 2002b), which leads to decreased duodenal iron uptake and increased reticuloendothelial macrophage iron sequestration (for a review, see Ganz, 2003). Additionally, downregulation of Fpn1 protein expression in the duodenum and reticuloendothelial macrophages in response to acute inflammatory stimuli (Yang et al., 2002) has been suggested to be mediated by Hamp-regulation of Fpn1 protein expression (Nicolas et al., 2002a; Nicolas et al., 2003). Furthermore, duodenal Fpn1 expression is responsive to systemic regulation, rather than to local iron levels (Chen et al., 2003). We provide strong in vivo evidence for this systemic effect, as high Fpn1 protein levels (Fig. 5C,D) correlate with low *Hamp* expression (Fig. 5F) at 7 weeks, whereas, by contrast, high levels of *Hamp* expression at 7 and 12 weeks (Fig. 5G) correlate with low Fpn1 protein expression (Fig. 5E). Furthermore, as *Fpn1* transcript levels appear unaffected in either 7- or 12-week-old livers (Fig. 5F,G), our data point to post-transcriptional regulation of *Fpn1* by Hamp, capable of achieving profound effects on Fpn1 protein levels, as evidenced by polycythemic heterozygotes at 7 weeks of age (Fig. 5D).

As downregulation of Fpn1 protein expression occurs normally in homozygous livers, despite the absence of an IRE in mutant *Fpn1* transcripts, our results suggest an IRE-independent mechanism of *Fpn1* regulation by Hamp. It has been suggested that transcriptional, in addition to post-transcriptional, mechanisms play an important role in regulating Fpn1 expression (Liu et al., 2002; Yang et al., 2002; Zoller et al., 2002; Chen et al., 2003). However, in the absence of appreciable differences in *Fpn1* transcript abundance (Fig. 5F), it is possible that a primarily post-transcriptional, IRE-independent mode of regulation leads to the profound differences in Fpn1 protein levels in *Pcm* mutant mice (Fig. 5C). Although the precise nature of this regulation is unknown, these data may point to a direct interaction between Fpn1 and Hamp proteins as a potential mechanism.

Based on our results, we propose that persistent Fpn1 expression caused by delayed postnatal *Hamp* upregulation forms the basis for the elevated iron uptake conducive for augmented erythropoiesis in *Pcm* mutant animals. As Hamp is a negative regulator of iron balance, and *Hamp* expression was upregulated by 12 weeks of age across all genotypes (Fig. 5G), further organismal accumulation of iron should cease and iron levels should decrease over time. Indeed, by 8-10 months of age, *Pcm* heterozygous mutants exhibited a significant decrease in hepatic iron content (Fig. 3E). This contrasts with the persistent iron accumulation in aged HFE- and *Hamp*-deficient animals (Nicolas et al., 2001; Lebeau et al., 2002; Nicolas et al., 2003). Importantly, chronic failure to induce *Hamp* expression in the context of iron overload has been shown to be the likely mechanism of dysregulated iron balance in HFE mutant mice (Ahmad et al., 2002; Nicolas et al., 2003). Conversely, return of hepatic iron content to baseline in aged *Pcm* heterozygotes (Fig. 3E) is indicative of intact Hamp regulation in *Pcm* mutant animals. Additionally, findings of anemia and low serum iron are consistent with Hamp-mediated, reticuloendothelial iron sequestration, similar to the anemia of chronic disease, also termed the anemia of inflammation (for a review, see Jurado, 1997).

Elevation of Epo expression observed in *Pcm* mutants rules out a primary polycythemia, such as polycythemia vera (for a review, see Prchal, 2001). Although the observed increase in Fpn1 protein expression would appear adequate to supply sufficient iron required for the augmented erythropoiesis in *Pcm* mutant animals, the observed polycythemia in *Pcm* heterozygous animals is most likely a secondary, Epo-dependent phenomenon. To explain the increased Epo expression observed in *Pcm* mutant mice that leads to the transient polycythemia, we propose a model by which increased Fpn1 protein expression and concomitant intracellular iron deficiency leads to Hamp downregulation. At birth, homozygous mutant animals are severely iron deficient, leading to hypochromic, microcytic anemia, while heterozygotes have decreased but sufficient iron stores, permitting near-wild-type Hct. Increased Fpn1 protein expression in *Pcm* mutants during early postnatal life, i.e. the primary effect of the microdeletion in the *Pcm* promoter region, causes augmented cellular iron efflux, e.g. in the liver and kidney, exacerbating further the cellular iron deficiency. This should lead to the following distinct molecular consequences in cell types involved in hypoxia and iron sensing:

In the first component of the model, cellular iron deficiency is known to mimic hypoxia (for a review, see Semenza, 1998), sensing of which requires an iron-dependent prolyl hydroxylase (Epstein et al., 2001; Ivan et al., 2001; Jaakkola et al., 2001). Thus, increased Fpn1-mediated iron efflux in hypoxia sensing cells in the liver and kidney leads to inappropriate induction of Epo expression, as observed at 3 weeks of age (Fig. 4A). This effect of increased Epo production is ineffective in homozygotes until the severe perinatal iron deficiency resolves as a consequence of increased Fpn1-mediated duodenal uptake during early postnatal development. By contrast, as sufficient iron for productive erythropoiesis is present, elevated Epo expression in heterozygotes results in

increased erythropoiesis. Although not fully defined as a clinical entity, mild but significant increases in red cell indices, including hematocrit, have indeed been observed in the context of iron deficiency in infants and young children (Aslan and Altay, 2003).

In the second component of the model, within the iron sensor of the liver (for a review, see Ganz, 2003), Fpn1-mediated efflux would be sensed as low cellular iron levels. In a regulatory response, this leads to repression of the negative hormonal regulator Hamp. Based on the concept that Hamp negatively regulates Fpn1 protein levels (Nicolas et al., 2002a; Nicolas et al., 2003), which is strongly supported by the present data, decreased Hamp expression would lead to further de-repression of Fpn1 protein levels in *Pcm* mutant animals, e.g. as seen at 7 weeks of age. This superimposed regulatory mechanism further exacerbates cellular iron deficiency in Fpn1-expressing cells. Concomitantly, in the duodenum, increase in Fpn1 protein expression driven by Hamp downregulation leads to increased iron absorption during early postnatal life in these mutants, culminating in tissue iron accumulation by 12 weeks of age (Fig. 3D,E). This represents a paradoxical state in which low iron levels are sensed cellularly, despite significant organismal iron accumulation in *Pcm* mutant animals. Additionally, recent data suggest Epo itself may downregulate *Hamp* expression (Nicolas et al., 2002c). Thus, *Hamp* downregulation in polycythemic *Pcm* mutant animals could be compounded by elevated Epo levels.

By 12 weeks of age, *Hamp* is upregulated across all genotypes, including the heterozygotes (Fig. 5G). This leads to decreased duodenal and reticuloendothelial Fpn1 protein expression, and, hence, decreased duodenal iron uptake and sequestration in the reticuloendothelial system. Over time, this would reduce organismal iron load, which is indeed observed in aged heterozygous mutant animal (Fig. 3E). The mechanism of *Hamp* upregulation in the heterozygous population observed at 12 weeks of age is unknown, yet correlates with return of *Epo* levels to baseline (Fig. 4E), and is indicative of the disruption of this feed-forward mechanism and reversion of the organismal phenotype over time. Hence, this dynamic model reconciles the molecular findings of Fpn1 and *Hamp* expression with the changes in iron homeostasis and aberrant erythropoiesis in *Pcm* mutant animals during postnatal development.

The significant iron deficiency observed at birth in *Pcm* mutants represents an unexpected finding relative to the augmented Fpn1-mediated organismal iron uptake that is characteristic of early postnatal life. Strikingly, our preliminary data reveal decreased Fpn1 expression in *Pcm* mutant placenta, consistent with the perinatal iron deficiency, and suggest differential developmental regulation of Fpn1 expression (H.M. and A.S., unpublished).

At present, it is unclear why the transient polycythemia is characteristic of the heterozygous as opposed to the homozygous mutant population. Perhaps in the absence of sufficient iron for productive erythropoiesis during crucial early postnatal timepoints, homozygotes are unable to undergo the significant erythropoiesis observed in heterozygous animals, despite upregulation of Epo expression during early postnatal development (Fig. 4B).

In summary, at birth, *Pcm* mutant animals are iron deficient. Owing to a gain-of-function mutation causing elevated Fpn1 protein levels in different cellular compartments postnatally, *Pcm* mutant animals display increased organismal iron uptake during early postnatal life, culminating in significant hepatic iron accumulation by young adulthood. Additionally, heterozygous mutant animals exhibit a transient polycythemia secondary to elevated Epo expression. *Hamp* upregulation by young adulthood correlates with downregulation of Fpn1 protein expression, preceding the reversion of the iron overload phenotype. Decreased Fpn1-mediated iron uptake in the duodenum abrogates organismal iron accumulation, while decreased Fpn1-mediated iron efflux from reticuloendothelial macrophages leads to sequestration, dynamically explaining the contrasting phenotypes during early postnatal and adult life in *Pcm* mutant mice.

We thank Drs Matthias Hentze, Bruno Galy and David Haile for generously providing Fpn1 antibody reagents; we are grateful to Drs Jeffrey Rosen and William Craigen, as well as members of our laboratory, for helpful discussions and critical reading of the manuscript. We acknowledge Sal Durrani for excellent technical assistance. H.M. is supported by an individual National Research Service Award from the National Institute of Environmental Health Sciences, NIH; has received NIH training grant support through the Department of Molecular and Human Genetics; and is a member of the Medical Scientist Training Program of Baylor College of Medicine funded by the NIH. This work was supported by a research grant from the NIH to A.S.

References

Abboud, S. and Haile, D. J. (2000). A novel mammalian iron-regulated protein involved in intracellular iron metabolism. *J. Biol. Chem.* **275**, 19906-19912.

Ahmad, K. A., Ahmann, J. R., Migas, M. C., Waheed, A., Britton, R. S., Bacon, B. R., Sly, W. S. and Fleming, R. E. (2002). Decreased liver hepcidin expression in the hfe knockout mouse. *Blood Cells Mol. Dis.* **29**, 361-366.

Ajioka, R. S. and Kushner, J. P. (2002). Hereditary hemochromatosis. *Semin. Hematol.* **39**, 235-241.

Aisen, P., Enns, C. and Wessling-Resnick, M. (2001). Chemistry and biology of eukaryotic iron metabolism. *Int. J. Biochem. Cell. Biol.* **33**, 940-959.

Andrews, N. C. (1999). The iron transporter DMT1. *Int. J. Biochem. Cell Biol.* **31**, 991-994.

Arden, K. E., Wallace, D. F., Dixon, J. L., Summerville, L., Searle, J. W., Anderson, G. J., Ramm, G. A., Powell, L. W. and Subramaniam, V. N. (2003). A novel mutation in ferroportin1 is associated with haemochromatosis in a Solomon Islands patient. *Gut* **52**, 1215-1217.

Aslan, D. and Altay, C. (2003). Incidence of high erythrocyte count in infants and young children with iron deficiency anemia: re-evaluation of an old parameter. *J. Pediatr. Hematol. Oncol.* **25**, 303-306.

Bannerman, R. M., Bannerman, C. E. and Kingston, P. J. (1973). Hereditary iron deficiency: X-linked anaemia (sla) in newborn and suckling mice. *Br. J. Haematol.* **25**, 280.

Bechensteen, A. G. and Halvorsen, S. (1996). Parenteral iron increases serum erythropoietin concentration during the 'early anaemia' of 10-20-day-old mice. *Br. J. Haematol.* **94**, 529-532.

Bernstein, S. E. (1987). Hereditary hypotransferrinemia with hemosiderosis, a murine disorder resembling human atransferrinemia. *J. Lab. Clin. Med.* **110**, 690-705.

Bondurant, M. C. and Koury, M. J. (1986). Anemia induces accumulation of erythropoietin mRNA in the kidney and liver. *Mol. Cell. Biol.* **6**, 2731-2733.

Cattanach, B. M. (1995). A dominant polycythaemia. *Mouse Genome* **93**, 1027-1028.

Cazzola, M., Cremonesi, L., Papaioannou, M., Soriani, N., Kioumi, A., Charalambidou, A., Paroni, R., Romtsou, K., Levi, S., Ferrari, M. et al. (2002). Genetic hyperferritinaemia and reticuloendothelial iron overload associated with a three base pair deletion in the coding region of the ferroportin gene (SLC11A3). *Br. J. Haematol.* **119**, 539-546.

Chen, H., Su, T., Attieh, Z. K., Fox, T. C., McKie, A. T., Anderson, G. J.

and Vulpe, C. D. (2003). Systemic regulation of Hephaestin and Ireg1 revealed in studies of genetic and nutritional iron deficiency. *Blood* **102**, 1893-1899.

Devalia, V., Carter, K., Walker, A. P., Perkins, S. J., Worwood, M., May, A. and Dooley, J. S. (2002). Autosomal dominant reticuloendothelial iron overload associated with a 3-base pair deletion in the ferroportin 1 gene (SLC11A3). *Blood* **100**, 695-697.

Donovan, A., Brownlie, A., Zhou, Y., Shepard, J., Pratt, S. J., Moynihan, J., Paw, B. H., Drejer, A., Barut, B., Zapata, A et al. (2000). Positional cloning of zebrafish ferroportin1 identifies a conserved vertebrate iron exporter. *Nature* **403**, 776-781.

Epstein, A. C., Gleadle, J. M., McNeill, L. A., Hewitson, K. S., O'Rouke, J., Mole, D. R., Mukherji, M., Metzen, E., Wilson, M. I., Dhanda, A. et al. (2001). C. elegans EGL-9 and mammalian homologs define a family of dioxygenases that regulate HIF by prolyl hydroxylation. *Cell* **107**, 43-54.

Finch, C. (1994). Regulators of iron balance in humans. *Blood* **84**, 1697-1702.

Fleming, R. E. and Sly, W. S. (2001). Ferroportin mutation in autosomal dominant hemochromatosis: loss of function, gain in understanding. *J. Clin. Invest.* **108**, 521-522.

Ganz, T. (2003). Hepcidin, a key regulator of iron metabolism and mediator of anemia of inflammation. *Blood* **102**, 783-788.

Girelli, D., Corrocher, R., Bisceglia, L., Olivieri, O., de Franceschi, L., Zelante, L. and Gasparini, P. (1995). Molecular basis for the recently described hereditary hyperferritinemia-cataract syndrome: a mutation in the iron-responsive element of ferritin L-subunit gene (the 'Verona mutation'). *Blood* **86**, 4050-4053.

Girelli, D., Corrocher, R., Bisceglia, L., Olivieri, O., Zelante, L., Panozzo, G. and Gasparini, P. (1997). Hereditary hyperferritinemia-cataract syndrome caused by a 29-base pair deletion in the iron responsive element of ferritin L-subunit gene. *Blood* **90**, 2084-2088.

Grosovsky, A. J., de Boer, J. G., de Jong, P. J., Drobetsky, E. A. and Glickman, B. W. (1988). Base substitutions, frameshifts, and small deletions constitute ionizing radiation-induced point mutations in mammalian cells. *Proc. Natl. Acad. Sci. USA* **226**, 245-252.

Hellman, N. E. and Gitlin, J. D. (2002). Ceruloplasmin metabolism and function. *Annu. Rev. Nutr.* **22**, 439-458.

Hentze, M. W. and Kuhn, L. C. (1996). Molecular control of vertebrate iron metabolism: mRNA-based regulatory circuits operated by iron, nitric oxide, and oxidative stress. *Proc. Natl. Acad. Sci. USA* **93**, 8175-8182.

Hentze, M. W., Caughman, S. W., Rouault, T. A., Barriocanal, J. G., Dancis, A., Harford, J. B. and Klausner, R. D. (1987). Identification of the iron-responsive element for the translational regulation of human ferritin mRNA. *Science* **238**, 1570-1573.

Ivan, M., Kondo, K., Yang, H., Kim, W., Valiando, J., Ohh, M., Salic, A., Asara, J. M., Lane, W. S. and Kaelin, W. G., Jr (2001). HIFalpha targeted for VHL-mediated destruction by proline hydroxylation: implications for O2 sensing. *Science* **292**, 464-468.

Jaakkola, P., Mole, D. R., Tian, Y. M., Wilson, M. I., Gielbert, J., Gaskell, S. J., Kriegsheim, A. V., Hebestreit, H. F., Mukherji, M., Schofield, C. J. et al. (2001). Targeting of HIF-alpha to the von Hippel-Lindau ubiquitylation complex by O2-regulated prolyl hydroxylation. *Science* **292**, 468-472.

Jouanolle, A. M., Douabin-Gicquel, V., Halimi, C., Loreal, O., Fergelot, P., Delacour, T., de Lajarte-Thirouard, A. S., Turlin, B., le Gall, J. Y., Cadet, E. et al. (2003). Novel mutation in ferroportin 1 gene is associated with autosomal dominant iron overload. *J. Hepatol.* **39**, 286-289.

Jurado, R. L. (1997). Iron, infections, and anemia of inflammation. *Clin. Infect. Dis.* **25**, 888-895.

Kina, T., Ikuta, K., Takayama, E., Wada, K., Majumdar, A. S., Weissman, I. L. and Katsura, Y. (2000). The monoclonal antibody TER-119 recognizes a molecule associated with glycophorin A and specifically marks the late stages of murine erythroid lineage. *Br. J. Haematol.* **109**, 280-287.

Knutson, M. and Wessling-Resnick, M. (2003). Iron metabolism in the reticuloendothelial system. *Crit. Rev. Biochem. Mol. Biol.* **38**, 61-88.

Lebeau, A., Frank, J., Biesalski, H. K., Weiss, G., Srai, S. K., Simpson, R. J., McKie, A. T., Bahram, S., Gilfillan, S. and Schumann, K. (2002). Long-term sequelae of HFE deletion in C57BL/6 x 129/O1a mice, an animal model for hereditary haemochromatosis. *Eur. J. Clin. Invest.* **32**, 603-612.

Liu, X., Hill, P. and Haile, D. J. (2002). Role of the ferroportin iron-responsive element in iron and nitric oxide dependent gene regulation. *Blood Cells Mol. Dis.* **29**, 315-326.

Means, R. T., Jr (2003). Recent developments in the anemia of chronic disease. *Curr. Hematol. Rep.* **2**, 116-121.

McKie, A. T., Marciani, P., Rolfs, A., Brennan, K., Wehr, K., Barrow, D., Miret, S., Bomford, A., Peters, T. J., Farzaneh, F. et al. (2000). A novel duodenal iron-regulated transporter, IREG1, implicated in the basolateral transfer of iron to the circulation. *Mol. Cell.* **5**, 299-309.

Miles, C. and Meuth, M. (1989). DNA sequence determination of gamma-radiation-induced mutations of the hamster aprt locus. *Mutat. Res.* **227**, 97-102.

Montosi, G., Donovan, A., Totaro, A., Garuti, C., Pignatti, E., Cassanelli, S., Trenor, C. C., Gasparini, P., Andrews, N. C. and Pietrangelo, A. (2001). Autosomal-dominant hemochromatosis is associated with a mutation in the ferroportin (SLC11A3) gene. *J. Clin. Invest.* **108**, 619-623.

Nicolas, G., Bennoun, M., Devaux, I., Beaumont, C., Grandchamp, B., Kahn, A. and Vaulont, S. (2001). Lack of hepcidin gene expression and severe tissue iron overload in upstream stimulatory factor 2 (USF2) knockout mice. *Proc. Natl. Acad. Sci. USA* **98**, 8780-8785.

Nicolas, G., Bennoun, M., Porteu, A., Mativet, S., Beaumont, C., Grandchamp, B., Sirito, M., Sawadogo, M., Kahn, A. and Vaulont, S. (2002a). Severe iron deficiency anemia in transgenic mice expressing liver hepcidin. *Proc. Natl. Acad. Sci. USA* **99**, 4596-4601.

Nicolas, G., Chauvet, C., Viatte, L., Danan, J. L., Bigard, X., Devaux, I., Beaumont, C., Kahn, A. and Vaulont, S. (2002b). The gene encoding the iron regulatory peptide hepcidin is regulated by anemia, hypoxia, and inflammation. *J. Clin. Invest.* **110**, 1037-1044.

Nicolas, G., Viatte, L., Bennoun, M., Beaumont, C., Kahn, A. and Vaulont, S. (2002c). Hepcidin, a new iron regulatory peptide. *Blood Cells Mol. Dis.* **29**, 327-335.

Nicolas, G., Viatte, L., Lou, D. Q., Bennoun, M., Beaumont, C., Kahn, A., Andrews, N. C. and Vaulont, S. (2003). Constitutive hepcidin expression prevents iron overload in a mouse model of hemochromatosis. *Nat. Genet.* **34**, 97-101.

Njajou, O. T., Vaessen, N., Joosse, M., Berghuis, B., van Dongen, J. W., Breuning, M. H., Snijders, P. J., Rutten, W. P., Sandkuijl, L. A., Oostra, B. A. et al. (2001). A mutation in SLC11A3 is associated with autosomal dominant hemochromatosis. *Nat. Genet.* **28**, 213-214.

Park, C. H., Valore, E. V., Waring, A. J. and Ganz, T. (2001). Hepcidin, a urinary antimicrobial peptide synthesized in the liver. *J. Biol. Chem.* **276**, 7806-7810.

Pigeon, C., Ilyin, G., Courselaud, B., Leroyer, P., Turlin, B., Brissot, P. and Loreal, O. (2001). A new mouse liver-specific gene, encoding a protein homologous to human antimicrobial peptide hepcidin, is overexpressed during iron overload. *J. Biol. Chem.* **276**, 7811-7819.

Prchal, J. T. (2001). Molecular biology of polycythemias. *Intern. Med.* **40**, 681-687.

Richardson, D. R. and Ponka, P. (1997). The molecular mechanisms of the metabolism and transport of iron in normal and neoplastic cells. *Biochim. Biophys. Acta.* **1331**, 1-40.

Rivard, S. R., Lanzara, C., Grimard, D., Carella, M., Simard, H., Ficarella, R., Simard, R., D'Adamo, A. P., de Braekeleer, M. and Gasparini, P. (2003). Autosomal dominant reticuloendothelial iron overload (HFE type 4) due to a new missense mutation in the FERROPORTIN 1 gene (SLC11A3) in a large French-Canadian family. *Haematologica*. **88**, 824-826.

Roetto, A., Papanikolaou, G., Politou, M., Alberti, F., Girelli, D., Christakis, J., Loukopoulos, D. and Camaschella, C. (2003). Mutant antimicrobial peptide hepcidin is associated with severe juvenile hemochromatosis. *Nat. Genet.* **33**, 21-22.

Roy, C. N. and Enns, C. A. (2000). Iron homeostasis: new tales from the crypt. *Blood* **96**, 4020-4027.

Semenza, G. L. (1998). Hypoxia-inducible factor 1 and the molecular physiology of oxygen homeostasis. *J. Lab. Clin. Med.* **131**, 207-214.

Torrance, J. D. and Bothwell, T. H. (1980). In *Iron* (ed. J. D. Cook), pp. 32-35, 90-115. New York: Churchill Livingstone.

Vulpe, C. D., Kuo, Y. M., Murphy, T. L., Cowley, L., Askwith, C., Libina, N., Gitschier, J. and Anderson, G. J. (1999). Hephaestin, a ceruloplasmin homologue implicated in intestinal iron transport, is defective in the sla mouse. *Nat. Genet.* **21**, 195-199.

Yang, F., Liu, X. B., Quinones, M., Melby, P. C., Ghio, A. and Haile, D. J. (2002). Regulation of reticuloendothelial iron transporter MTP1 (Slc11a3) by inflammation. *J. Biol. Chem.* **277**, 39786-39791.

Zhang, J., Socolovsky, M., Gross, A. W. and Lodish, H. F. (2003). Role of Ras signaling in erythroid differentiation of mouse fetal liver cells: functional analysis by a flow cytometry-based novel culture system. *Blood* **102**, 3938-3946.

Zoller, H., Theurl, I., Koch, R., Kaser, A. and Weiss, G. (2002). Mechanisms of iron mediated regulation of the duodenal iron transporters divalent metal transporter 1 and ferroportin 1. *Blood Cells Mol. Dis.* **29**, 488-497.